THE JOURNAL OF PHYSICAL CHEMISTRY C

Article

pubs.acs.org/JPCC

In Situ Soft X-ray Absorption Spectroscopy Applied to Solid–Liquid Heterogeneous Cyanopyrazine Hydration Reaction on Titanium Oxide Catalyst

Hayato Yuzawa,[†] Masanari Nagasaka,[†,‡] and Nobuhiro Kosugi*[,†,‡]

[†]Institute for Molecular Science, Myodaiji, Okazaki 444-8585, Japan

[‡]The Graduate University for Advanced Studies, Myodaiji, Okazaki 444-8585, Japan

Supporting Information

ABSTRACT: In conventional *in situ* spectroscopies of solid–liquid heterogeneous catalytic reactions, it is difficult to measure the conversion of liquid substrates on solid catalysts due to the lack of sensitivity and the difficulty in separation of target signals in the mixture of substrates, reactants, products, solvents, and solid catalysts. Element-specific soft X-ray absorption spectroscopy (XAS) is a promising method to detect target substrate and product separately from the other components using chemically different inner shell excitation energies. In the present work, we have developed an *in situ* sample cell to measure time- and temperature-dependent XAS spectra in transmission mode and applied it to one of the solid–liquid heterogeneous catalytic reactions, cyanopyrazine (PzCN) hydration to produce pyrazinamide ($PzCONH_2$) on the TiO_2 catalyst ($PzCN + H_2O \rightarrow PzCONH_2$). We have succeeded in unambiguous observation of the spectral change in the C K-edge and N K-edge XAS due to the production of $PzCONH_2$ from PzCN during the reaction regardless of the coexistence of the bulk liquid components, H_2O (reactant) and EtOH (solvent). Furthermore, we have obtained reasonable kinetic properties in the PzCN hydration reaction from the spectral analysis such as the reaction order (first order), the rate constant, and the activation energy. Thus, the present method can be widely applicable to distinguish the minor liquid components in chemical reactions.

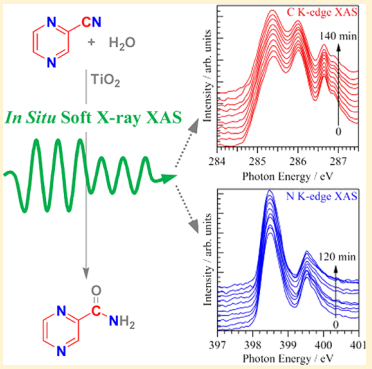

1. INTRODUCTION

Investigation of the catalytic reaction mechanism is important to obtain some clue to improvements of catalyst activity, selectivity, durability, and so on. Spectroscopic observation under the reaction condition (*in situ* spectroscopy) is one of the most effective ways to elucidate the mechanism. However, *in situ* spectroscopy for solid–liquid heterogeneous catalytic reactions (liquid phase reaction on solid catalyst) is generally difficult to measure due to interface phenomena between two condensed phases, which hinder the objective spectral change through the absorption of the probe light.[1,2]

In situ spectroscopy of catalysis has been used to study two types of targets; one is the transformation cycle of the catalyst, and the other is the conversion process from the substrate to the product. In the former type for the solid–liquid heterogeneous catalytic reaction, hard X-ray XAS has been typically used.[3−6] In this target, the energy regions of the absorption light for liquid substrates and for solid catalysts are generally separable because the substrates are mostly composed of light elements (C, N, O, etc.), and the solid catalysts contain heavier elements (metal elements). Since the reaction proceeds with the conversion cycle of the surface structure on the catalyst, the spectral change derived from the catalytic cycle is mainly observed from the photoabsorption of the (near) surface. The photoabsorption of the internal bulk solid structure of the catalyst is a main hindrance in obtaining the target spectral change. Fortunately, the present catalytic reaction system can reduce this hindrance because the present nanoparticle catalysts have a higher ratio of surface vs bulk.

On the other hand, in the latter type for the solid–liquid heterogeneous catalytic reaction, NMR[7−9] and attenuated total reflection IR (ATR-IR)[10−14] have been frequently used. In this target, since liquid substrate is usually diluted by solvent and other reactants, the observation of minor liquid component in the reaction system is highly required. However, these methods have different drawback for the detection of minor liquid substrates. The NMR measurement requires low natural abundance isotope atoms in most of light elements, and the sensitivity is inevitably low for minor components.[15] In the ATR-IR, many absorption peaks assigned to various vibration modes exhibit similar wavenumbers, and the objective peaks of minor liquid components are often hindered by other liquid components. The lack of sensitivity and the difficulty in separation of target peaks make difficult the *in situ* measurement of solid–liquid heterogeneous catalytic reactions. Thus, new methodologies are still required for the *in situ* observation of the liquid substrate conversion on the solid catalyst in the realistic condition.

Received: December 26, 2014
Revised: March 19, 2015
Published: March 20, 2015

DOI: 10.1021/jp512891t
J. Phys. Chem. C 2015, 119, 7738−7745

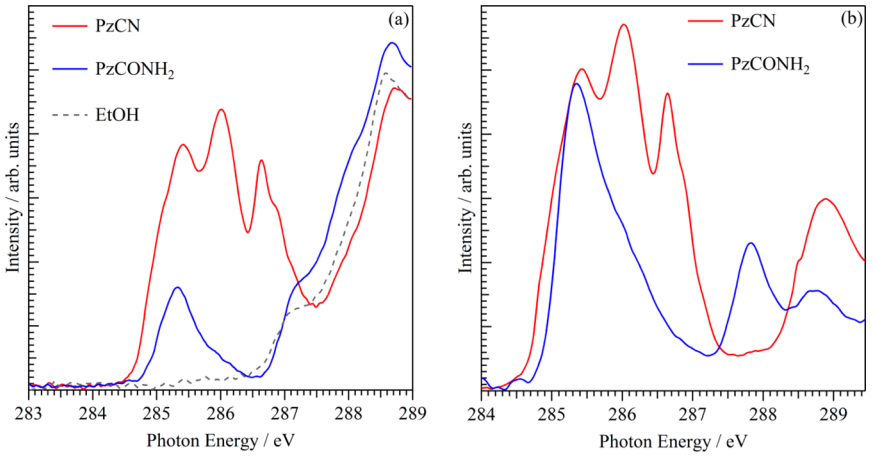

Figure 1. (a) C K-edge XAS spectra of the suspension of PzCN (red line) and $PzCONH_2$ (blue line) and (b) those of the saturated aqueous solution measured at 298 K. In panel a, the PzCN suspension contains 0.78 M of PzCN, 2.0 M of EtOH, 45 M of H_2O, and 3.5 mg/mL of TiO_2, and the $PzCONH_2$ suspension contains 0.19 M of $PzCONH_2$, 43 M of H_2O, 4.0 M of EtOH, and 3.5 mg/mL of TiO_2. Gray dashed line in panel a is the C K-edge XAS spectrum of pure EtOH.

XAS in the soft X-ray region is a powerful tool to observe local structures of the light elements in various molecular systems. This method has been already applied to the observation of catalytic reactions such as C K-edge XAS observations of benzene oxidation on Pt(111) surface,[16] water-gas shift reaction on CeO_x/Au(111),[17] and $L_{2,3}$ edges of Co and Mn XAS observation of reduction behavior for Co/Mn/TiO_2 catalysts under Fischer–Tropsch synthesis.[18] However, those targets are only either gas phase substrates or solid catalysts, and the conversion of liquid substrates on the solid catalyst has not yet been investigated. Since soft X-rays are strongly absorbed by light elements such as C, N, and O, it is highly required that the soft X-rays pass through thin liquid samples below a few micrometers thickness under the vacuum condition.[19] XAS in transmission mode is a quantitative method to measure the absolute photoabsorption cross section.

XAS spectra of liquid samples can be measured by various methods, not only transmission mode[20] but also fluorescence yield,[21] nonresonant Raman scattering process,[22] total electron yield of liquid microjet,[23] and inverse partial fluorescence yield of liquid microjet.[24−27] The latter methods are based on secondary processes, proportional to the probability of the core hole creation following the X-ray absorption. Their compatibility with the transmission measurement has been discussed as regards background subtraction, normalization, and saturation correction. Note that XAS in bulk liquid phase measured by the nonresonant Raman scattering and the inverse partial fluorescence yield is nearly the same as XAS in transmission mode. The XAS in transmission mode is an effective and simplest method to measure the time dependence of local structural change in bulk liquid[28] and is easily applicable to temperature-dependent measurements,[29] which is essential for the analysis of catalytic reaction.

Recently, a liquid flow cell in transmission mode has been successfully developed.[30] This liquid cell with two Si_3N_4 or SiC membranes is able to control the thickness of the liquid sample from 20 to 2000 nm under ambient pressure. By using this cell, we have revealed the local structure of methanol–water binary solutions from the C and O K-edge XAS[31] and the process of electrochemical redox reaction of Fe ions in aqueous solutions from the Fe L-edge XAS.[32,33]

In the present study, we have applied this *in situ* transmission cell to the time- and temperature-dependent soft X-ray absorption measurement of the solid–liquid heterogeneous catalytic reaction. It is well-known that the nitrile hydration on solid catalysts selectively proceeds to give the corresponding amide.[34−38] Furthermore, since small particles of solid catalysts dispersed in liquid have large areas in the solid–liquid interface, the transmission mode can be an effective method for the measurement of the solid–liquid interface. Thus, we have chosen the hydration reaction of cyanopyrazine (PzCN) to produce pyrazinamide ($PzCONH_2$) on the TiO_2 nanoparticle catalyst (eq 1) as an appropriate reaction for the first demonstration of *in situ* measurement for the solid–liquid heterogeneous catalytic reaction by using soft X-ray absorption spectroscopy in transmission mode. In this reaction system, we have investigated the kinetics by the C K-edge and N K-edge XAS of liquid PzCN under the catalytic reaction.

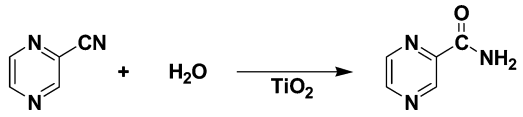

(1)

2. EXPERIMENTAL SECTION

2.1. Reagents. TiO_2 sample, JRC-TIO-4 (anatase/rutile, 50 ± 15 $m^2\ g^{-1}$), was supplied by Catalysis Society of Japan. Other reagents were PzCN (TCI, >97%), $PzCONH_2$ (TCI, >98%), and EtOH (Wako, 99.5%). All these reagents were used without further purification.

2.2. Apparatus of Soft X-ray Beamline. The experiments were carried out on an in-vacuum soft X-ray undulator beamline BL3U in UVSOR-III Synchrotron. The beamline and the liquid cell for the transmission mode were previously described in detail.[30,39] The liquid cell consists of two Si_3N_4 membranes for C K-edge XAS or SiC membranes for N K-edge XAS (NTT AT Co., Ltd., thickness: 100 nm, window size: 2 × 2 mm) and two Teflon spacers (thickness: 100 μm). Soft X-rays under vacuum (region I) pass through the buffer region filled with He gas (region II) and the liquid thin layer (region III) and finally reach a photodiode detector filled with He gas (region IV). The regions II and IV are connected and can be mixed with other gas molecules for the simultaneous photon energy calibration. The region I in vacuum and the region II and IV in He atmosphere are separated by another Si_3N_4 or SiC membrane (thickness: 100 nm; window size: 0.2 × 0.2 mm). A liquid sample (region III) is sandwiched between the two membranes (Si_3N_4 or SiC) with pressed the Teflon spacers can be substituted by other samples with a tubing pump system. The thickness of the liquid cell (the gap between the two membranes) can be controlled from 2000 to 20 nm with increasing the flowing He pressure in the regions II and IV.

DOI: 10.1021/jp512891t
J. Phys. Chem. C 2015, 119, 7738−7745

The temperature of liquid sample in the cell is controlled by the circulation of a liquid heat carrier, Nybrine Z-1 (MORESCO, main component: ethylene glycol), around the cell from a thermo-chiller, and it is monitored by a thermopile.

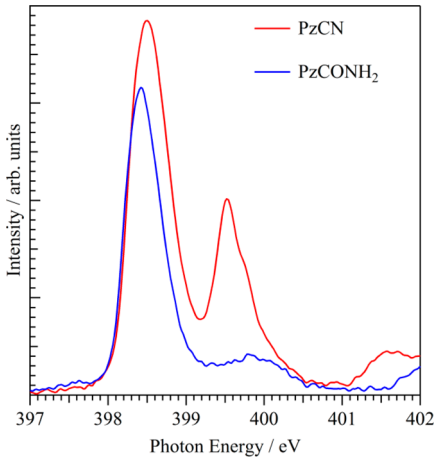

Figure 2. N K-edge XAS spectra of the suspension of PzCN (red line) and $PzCONH_2$ (blue line) measured at 298 K. The former suspension contains 0.78 M of PzCN, 2.0 M of EtOH, 45 M of H_2O, and 3.5 mg/mL of TiO_2, and the latter suspension contains 0.19 M of $PzCONH_2$, 43 M of H_2O, 4.0 M of EtOH, and 3.5 mg/mL of TiO_2.

2.3. *In Situ* Soft X-ray Absorption Spectroscopy of Catalytic Reactions. Suspension of the catalytic hydration reaction is prepared by 3.0 mL of PzCN (0.78 M), 35 mL of H_2O (45 M), 5.0 mL of EtOH (2.0 M), and 0.15 g of TiO_2 catalyst (3.5 mg/mL). The mixture is stirred by a magnetic stirrer for 10 min, followed by the sonication for 30 min to disperse the TiO_2 catalyst. After the liquid cell filled with 2.0 M aqueous EtOH containing 3.5 mg/mL of TiO_2 in advance is heated to the reaction temperature (323.2−344.5 K), the 20 mL of suspension is flowed into the liquid cell at 5.0 mL/min by using the tubing pump. Then, the measurement of the C K-edge or N K-edge XAS is started simultaneously with the stop of the flowing. In this procedure, the temperature of the reaction cell is lower by 4−5 K than the objective one at the start of the measurement because the prepared suspension (ca. 298 K) is not heated in advance. However, since the liquid cell volume is very small (at most 1.6×10^{-4} mL) and the temperature of the reaction system is recovered within 2 min, this decrease in temperature seriously did not influence on the entire measurements. In the *in situ* C K-edge XAS, the energy scan of soft X-rays from 283 to 289 eV, which takes 14 min, was repeated ten times (totally 140 min) at four different temperatures (323.2, 328.8, 335, and 338.5 K). In the *in situ* N K-edge XAS, the energy scan of soft X-rays from 397 to 402 eV, which takes 12 min, was repeated ten times (120 min) at three different temperatures (325.1, 331.3, and 344.5 K). The incident photon energies in the C K-edge XAS and N K-edge XAS were calibrated by the C 1s → 3 pt_2

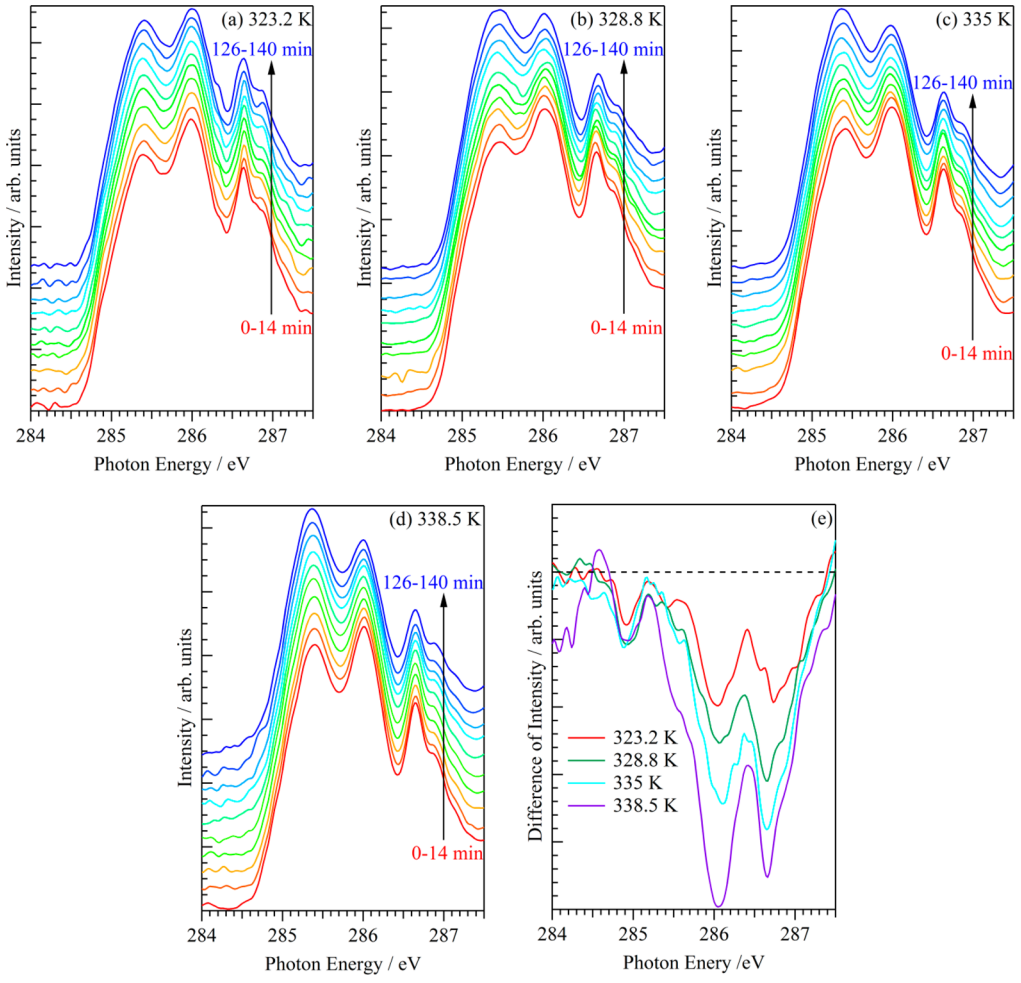

Figure 3. *In situ* C K-edge XAS spectra of the PzCN hydration reaction on the TiO_2 catalyst at (a) 323.2, (b) 328.8, (c) 335, and (d) 338.5 K and (e) difference spectra between the final (126−140 min) and the first energy scan (0−14 min) at each temperature. Dashed line in panel e shows the zero-difference intensity. Each spectrum was measured from 283 to 289 eV for 14 min and shows the observable energy region of the absorption for PzCN and $PzCONH_2$ (284−287.5 eV). Catalyst (TiO_2), 3.5 mg/mL; PzCN, 0.78 M; H_2O, 45 M; EtOH (solvent), 2.0 M.

DOI: 10.1021/jp512891t
J. Phys. Chem. C 2015, 119, 7738−7745

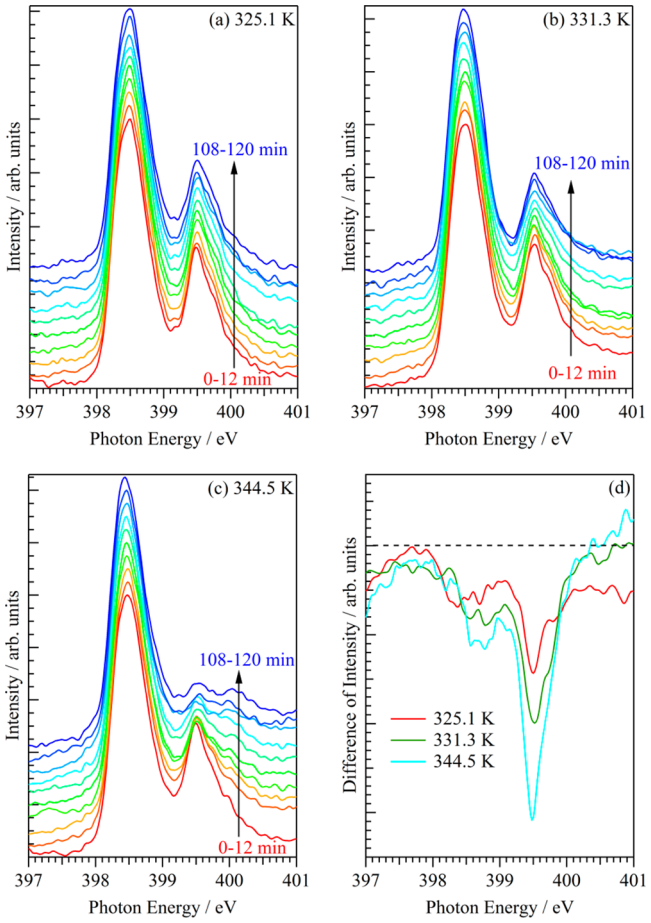

Figure 4. *In situ* N K-edge XAS spectra of the PzCN hydration reaction on the TiO_2 catalyst at (a) 325.1, (b) 331.3, and (c) 344.5 K and (e) difference spectra between the final (108−120 min) and the first energy scan (0−12 min) at each temperature. Dashed line in panel d shows the zero-difference intensity. Each spectrum was measured from 397 to 402 eV for 12 min and shows the observable energy region of the absorption for PzCN and $PzCONH_2$ (397−401 eV). Catalyst (TiO_2), 3.5 mg/mL; PzCN, 0.78 M; H_2O, 45 M; EtOH (solvent), 2.0 M.

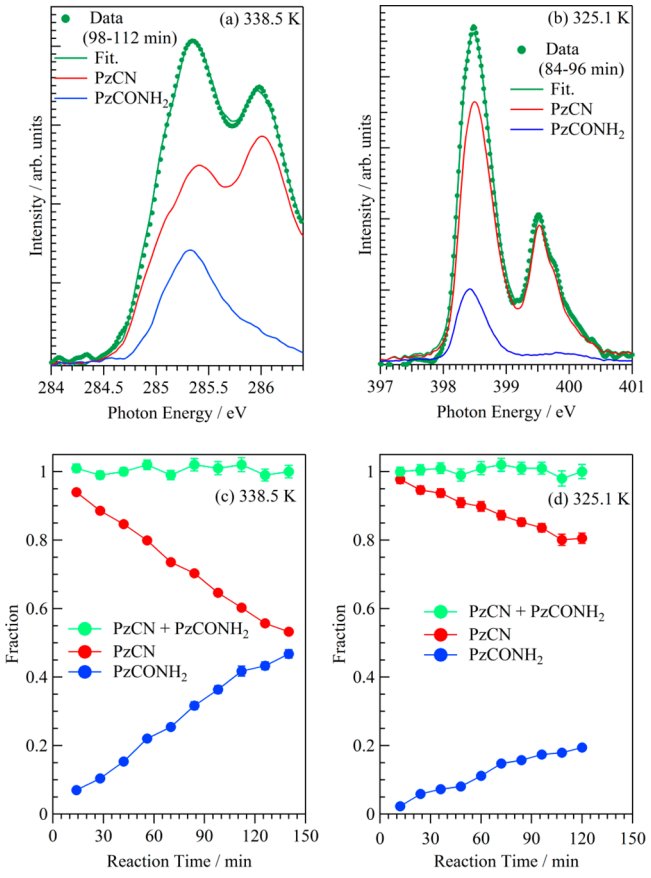

Figure 5. Fitting analyses for (a) the energy scan of the *in situ* C K-edge XAS spectrum from 98 to 112 min at 338.5 K and (b) that of the *in situ* N K-edge XAS spectrum from 84 to 96 min at 325.1 K of the PzCN hydration reaction on the TiO_2 catalyst and (c) the obtained fractions of PzCN and $PzCONH_2$ from the C K-edge XAS spectra at 338.5 K (Figure 3d) and (d) that from the N K-edge XAS spectra at 325.1 K (Figure 4a).

Rydberg peak of free CH_4 molecules (287.99 eV)[40] and N 1s → π^* peak of free N_2 molecules (400.84 eV),[41] respectively.

3. RESULTS AND DISCUSSION

3.1. *In Situ* C K-Edge and N K-Edge XAS. Figure 1 shows the C K-edge XAS spectra of PzCN and $PzCONH_2$ suspensions containing H_2O, solvent EtOH and TiO_2 (Figure 1a), and those of the saturated aqueous solution (Figure 1b) at room temperature (298 K). In the spectrum of PzCN suspension (Figure 1a, red line), three absorption peaks (285.4, 286.0, and 286.6 eV) are observed except for the absorption of EtOH (see the XAS spectrum of EtOH in gray dashed line). The two peaks at the lower photon energies (285.4 and 286.0 eV) are assigned to the excitations of carbons in the pyrazine ring from 1s to two π^* orbitals at different energy levels according to previous studies of NEXAFS for pyrazine.[42,43] The highest energy peak (286.6 eV) corresponds to the excitation of carbon in the cyano group from 1s to $\pi^*_{C\equiv N}$ orbital.[44] On the other hand, in the spectrum of $PzCONH_2$ suspension (Figure 1a, blue line), one broad asymmetric shaped absorption peak (285.3 eV) is only observed in the energy region of carbon in the pyrazine ring. Although the absorption from C 1s to another π^* orbital in pyrazine ring (288.9 eV for PzCN and 288.7 eV for $PzCONH_2$) and that from C 1s to $\pi^*_{C=O}$ in the amide group for $PzCONH_2$ (287.8 eV) are actually observed (Figure 1b), it gets covered up by the absorption of EtOH.

Figure 2 shows the N K-edge XAS spectra of the PzCN and $PzCONH_2$ suspensions. PzCN (red line) exhibits two absorption peaks at 398.5 and 399.5 eV; the 398.5 eV peak is the excitation from N 1s to π^*orbital in the pyrazine ring,[42,43] and the 399.5 eV peak is the excitation from N 1s to $\pi^*_{C\equiv N}$ orbital in the cyano group.[44] $PzCONH_2$ (blue line) exhibits only the former peak (398.4 eV) in this energy region. The absorption from N 1s to $\pi^*_{C=O}$ orbital in the amide group has been reported in various amide compounds, e.g., formamide[45] and malonamide.[46] In Figure 2, a very small absorption peak corresponding to $\pi^*_{C=O}$ is also observed around 400 eV.[15]

All the absorption peaks observed in the C K-edge XAS (Figure 1) and N K-edge XAS (Figure 2) do not change in this measurement condition for at least 180 min, which is longer than the investigated catalytic reaction time (120 or 140 min) in the present study. This confirms that the subsequent conversion of PzCN observed as some spectral changes is not derived from the excitation of the substrate molecules or photocatalysis of TiO_2 induced by soft X-rays.

It is notable that XAS can clearly detect the absorption peaks of PzCN and $PzCONH_2$ although these components are minor in the prepared suspensions. We have clearly demonstrated that this fact is profitable by comparing the result of XAS with that of

DOI: 10.1021/jp512891t
J. Phys. Chem. C 2015, 119, 7738−7745

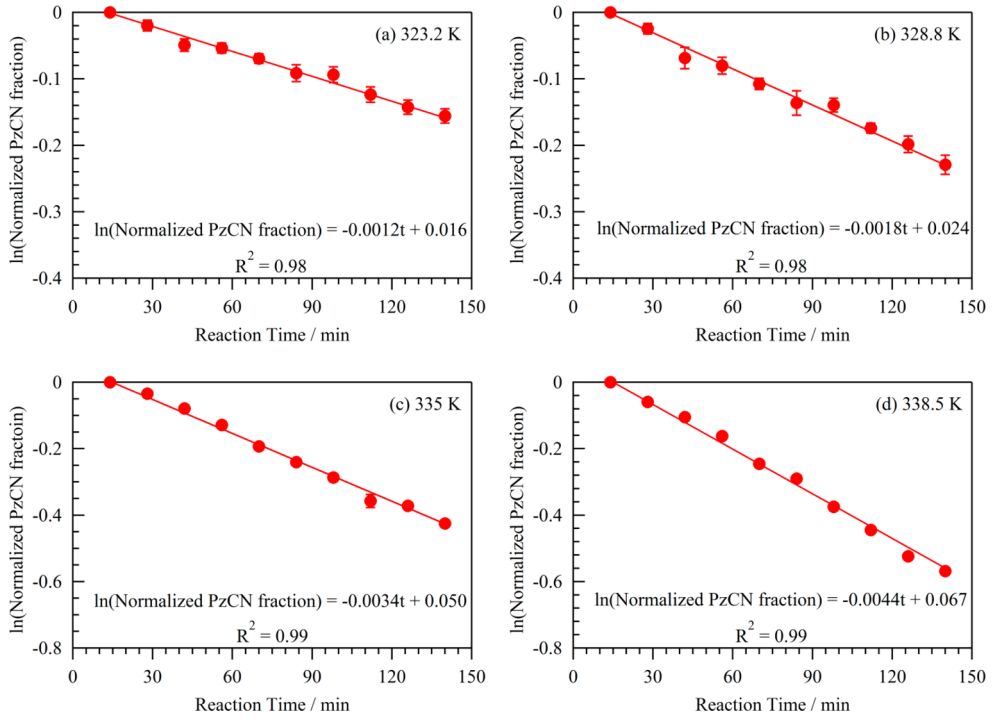

Figure 6. Logarithmic plots of the PzCN fraction obtained from the fitting analysis (Figure 5) for the *in situ* C K-edge XAS spectra of the PzCN hydration reaction on the TiO_2 catalyst at (a) 323.2, (b) 328.8, (c) 335, and (d) 338.5 K.

FT-IR spectroscopy. Figure S1 shows the obtained spectra of pure PzCN and PzCN solution without the TiO_2 catalyst by using the same liquid sample cell. In the present study, the obtained FT-IR spectrum in transmission mode can give equivalent information to that in ATR-IR, which is the most commonly used for the solid−liquid heterogeneous catalytic reactions. This is because the liquid cell used in the measurement can control the thickness from 20 to 2000 nm, which is a similar value for the penetration depth of evanescent IR light in ATR-IR. As a result, FT-IR cannot detect the absorptions of PzCN (C−H stretching and C≡N stretching mode) in the present condition (Figure S1b). This is not because the intensities of the objective absorption peaks are lower than each detection limit for the FT-IR spectrometer but because they are inhibited by the other components (H_2O and EtOH). Thus, XAS has proved to have an advantage to separate absorption peaks of minor components in the present reaction system.

Figures 3 and 4 show *in situ* C K-edge XAS spectra of the PzCN hydration reaction on the TiO_2 catalyst at 323.2 (Figure 3a), 328.8 (b), 335 (c) and 338.5 K (d) and *in situ* N K-edge XAS spectra at 325.1 (Figure 4a), 331.3 (b), and 344.5 K (c). All the obtained *in situ* spectra in Figures 3 and 4 vary the ratio of the absorption peak intensities of PzCN with the reaction time. Furthermore, as shown in the difference spectra between the final and the first energy scans at each temperature (Figures 3e and 4d), the spectral variation rate increases with increasing the reaction temperature. These results clearly indicate that the conversion of the minor component, PzCN, can be successfully detected as the spectral change.

When the fitting analysis of the obtained spectra is carried out, the observed variation is derived from whether the production of the objective compound or not. Figures 5a and 5b show examples of fitting analysis for the obtained *in situ* C K-edge and N K-edge XAS spectra (Figures 3 and 4) by using the reference spectra of PzCN and $PzCONH_2$ in Figures 1a and 2. In the C K-edge XAS, since the absorption peak of EtOH is observed in the energy region higher than 286.4 eV (Figure 1a), the fitting analyses have been carried out in the energy region from 284 to 286.4 eV. As a result, all of the *in situ* spectra, except for the energy scans of the *in situ* N K-edge XAS from 84 to 120 min at 344.5 K (Figure 4c) with too small contributions from PzCN, are well fitted by the reference spectra although the spectra should change continuously with the reaction time. This would be because the rate of spectral change, i.e., the hydration reaction rate, was relatively small for the energy scan time of the fitting energy region (5.6 min for the C K-edge XAS from 284 to 286.4 eV and 9.6 min for the N K-edge XAS from 397 to 401 eV). Figures 5c and 5d show the fractions of PzCN and $PzCONH_2$ obtained from the fitted ratio to the reference absorption spectra. The sum of two components is almost constant (0.96−1.04) and is not time dependent. This indicates each spectrum may be regarded as a spectrum measured every 14 min for the C K-edge XAS and every 12 min for the N K-edge XAS. Thus, Figure 5 definitely shows the conversion process from the substrate PzCN to the product $PzCONH_2$.

3.2. Kinetics. From the obtained fractions of PzCN and $PzCONH_2$ with the soft X-ray XAS, we have carried out the kinetic analysis of the PzCN hydration reaction on the TiO_2 catalyst. Figures 6 and 7 show the logarithmic plots of the normalized fractions of PzCN in Figure 5 for reaction time at each reaction temperature. All of the plots at each temperature clearly exhibit a linear relationship.

Considering the reaction mechanism of nitrile hydration on metal oxides reported in previous studies,[34−38] the reaction rate is able to describe as a first order rate eq 2 in the present condition (a detailed explanation about the rate equation of PzCN hydration reaction is shown in the Supporting Information).

$$\frac{d[PzCN]}{dt} = -\frac{k_3 K_1 K_2 C_{H_2O}}{(1 + K_2 C_{H_2O})^2}[PzCN] \quad (2)$$

DOI: 10.1021/jp512891t
J. Phys. Chem. C 2015, 119, 7738−7745

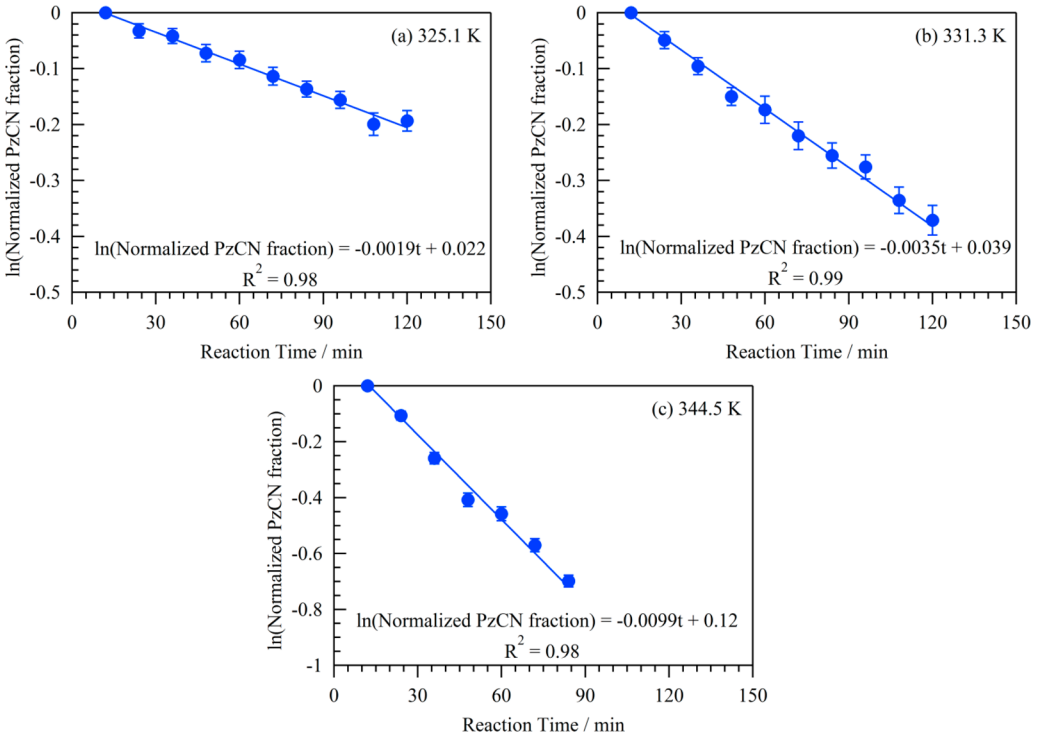

Figure 7. Logarithmic plots of the PzCN fraction obtained from the fitting analysis (Figure 5) for the *in situ* N K-edge XAS spectra of the PzCN hydration reaction on the TiO_2 catalyst at (a) 325.1, (b) 331.3, and (c) 344.5 K.

K_1, K_2, k_3, and C_{H_2O} correspond to the equilibrium constant for the adsorption of PzCN, that for the adsorption of H_2O on TiO_2 surface, the rate constant for the reaction between PzCN and H_2O adsorbed on TiO_2 surface, and the constant concentration of H_2O, respectively. From eq 2, the relationship between the concentration of PzCN and reaction time is led to the following eq 3, which is consistent with the form of the linear relationship in Figures 6 and 7.

$$\ln \frac{[\mathrm{PzCN}]}{[\mathrm{PzCN}]_0} = \ln(\text{normalized PzCN fraction}) = -\frac{k_3 K_1 K_2 C_{H_2O}}{(1 + K_2 C_{H_2O})^2} t \quad (3)$$

Thus, the gradients of the logarithmic plots in Figures 6 and 7 are expected to be the apparent rate constants corresponding to $k_3K_1K_2C_{H_2O}/(1 + K_2C_{H_2O})^2$ at each temperature.

Since the nitrile hydration on the solid catalyst has a single value of the activation energy in the region of our reaction temperatures,[37] the Arrhenius plot obtained from the rate constant of the hydration reaction should show a linear dependence on $1/T$. In Figures 6 and 7, the rate constant is determined as a gradient of the logarithmic plot for the fraction of the PzCN obtained from the *in situ* C K-edge and N K-edge XAS. In Figure 8, the Arrhenius plots using the obtained rate constants show a linear dependence. Then, the apparent activation energy can be evaluated, and the resultant values 77 kJ/mol (C K-edge) and 80 kJ/mol (N K-edge) are comparable with those of the benzonitrile hydration reaction on $Ru(OH)_x/Al_2O_3$ catalyst (71.5 kJ/mol)[35] and the cyanopyridine hydration reaction on CeO_2 catalyst (81.7 kJ/mol for 2-cyanopyridine and 80.7 kJ/mol for 4-cyanopyridine).[37] Therefore, the obtained rate constants from Figures 6 and 7 are verified as reasonable values.

The activation energy from the *in situ* N K-edge XAS is almost the same as that from the C K-edge XAS; on the other hand, the rate constants from the N K-edge XAS are about 20% larger than

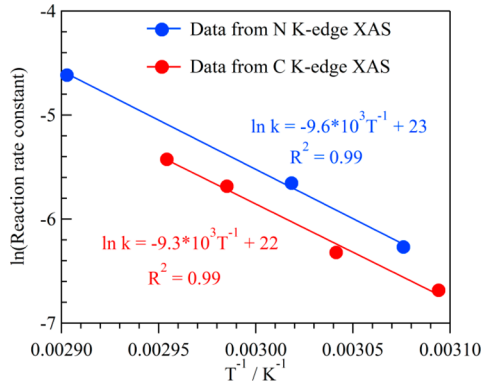

Figure 8. Arrhenius plots for the PzCN hydration reaction on the TiO_2 catalyst based on the gradient of logarithmic plots for the PzCN fraction in Figures 6 and 7. Red and blue circles correspond to the data from the C K-edge XAS and the N K-edge XAS, respectively.

those from the C K-edge XAS, as clearly recognized in Figure 8. This systematic difference in the rate constant may arise from a different experimental condition; namely, different liquid cells for the C K-edge XAS (Si_3N_4 membrane) and for the N K-edge XAS (SiC membrane). Since TiO_2 catalyst was still imperfectly dispersed into the PzCN solution even after the sonication, TiO_2 particles are deposited to some extent on the membrane surface under the suspension flowing before starting the measurement. The liquid cell of SiC membrane for the N K-edge XAS would contain larger quantity of TiO_2 catalysts and exhibit the higher reaction rate.

4. CONCLUSION

We have successfully performed *in situ* observation of the solid–liquid heterogeneous catalytic reaction, PzCN hydration reaction

DOI: 10.1021/jp512891t
J. Phys. Chem. C 2015, 119, 7738–7745

on TiO_2, by using soft X-ray absorption spectroscopy in transmission mode.

(i) Compared with the commonly used spectroscopies (e.g., ATR-IR, NMR), the merit of this method for the PzCN hydration reaction is the separable detection of the conversion of the minor liquid component under the reaction condition. Especially, the hindrance of bulk liquid water can be perfectly removed. Furthermore, separation of the minor component is more advantageous when the substrate organic compound contains heteroatoms (N atom in this study). (ii) Analyses of the *in situ* spectra can give the information about the reaction kinetics (rate order and constant and activation energy).

In the future, we will try to detect the interaction between liquid substrate and solid catalyst, intermediate species, and the effect of solvent under the reaction.

■ ASSOCIATED CONTENT

Supporting Information

Comparison of soft X-ray XAS with FT-IR spectroscopy in the PzCN solution and the pure PzCN (Figure S1); explanation of rate equation for PzCN hydration reaction based on its reaction mechanism (Figure S2). This material is available free of charge via the Internet at http://pubs.acs.org.

■ AUTHOR INFORMATION

Corresponding Author

*E-mail: kosugi@ims.ac.jp (N.K.).

Notes

The authors declare no competing financial interest.

■ ACKNOWLEDGMENTS

We thank the staff members of the UVSOR-III facility for their kind support. This work was financially supported by JSPS Grants-in-Aid for Scientific Research (A) (Grants 23245007 and 26248010), that for Young Scientists (B) (26810010), and that for JSPS fellows (26-7798).

■ REFERENCES

(1) Zaera, F. Surface Chemistry at the Liquid/Solid Interface. *Surf. Sci.* **2011**, *605*, 1141−1145.

(2) Zaera, F. Probing Liquid/Solid Interfaces at the Molecular Level. *Chem. Rev.* **2012**, *112*, 2920−2986.

(3) Ellis, P. J.; Fairlamb, I. J. S.; Hackett, S. F. J.; Wilson, K.; Lee, A. F. Evidence for the Surface-Catalyzed Suzuki−Miyaura Reaction over Palladium Nanoparticles: An Operando XAS Study. *Angew. Chem., Int. Ed.* **2010**, *49*, 1820−1824.

(4) Reimann, S.; Stötzel, J.; Frahm, R.; Kleist, W.; Grunwaldt, J.-D.; Baiker, A. Identification of the Active Species Generated from Supported Pd Catalysts in Heck Reactions: An in situ Quick Scanning EXAFS Investigation. *J. Am. Chem. Soc.* **2011**, *133*, 3921−3930.

(5) Friebel, D.; Miller, D. J.; Nordlund, D.; Ogasawara, H.; Nilsson, A. Degradation of Bimetallic Model Electrocatalysts: An In Situ X-ray Absorption Spectroscopy Study. *Angew. Chem., Int. Ed.* **2011**, *50*, 10190−10192.

(6) Karim, A. M.; Howard, C.; Roberts, B.; Kovarik, L.; Zhang, L.; King, D. L.; Wang, Y. In Situ X-ray Absorption Fine Structure Studies on the Effect of pH on Pt Electronic Density during Aqueous Phase Reforming of Glycerol. *ACS Catal.* **2012**, *2*, 2387−2394.

(7) Bellière, V.; Lorentz, C.; Geantet, C.; Yoshimura, Y.; Laurenti, D.; Vrinat, M. Kinetics and Mechanism of Liquid-Phase Alkylation of 3-Methylthiophene with 2-Methyl-2-butene over a Solid Phosphoric acid. *Appl. Catal., B* **2006**, *64*, 254−261.

(8) Huang, J.; Long, W.; Agrawal, P. K.; Jones, C. W. Effects of Acidity on the Conversion of the Model Bio-oil Ketone Cyclopentanone on H-Y Zeolites. *J. Phys. Chem. C* **2009**, *113*, 16702−16710.

(9) Vjunov, A.; Hu, M. Y.; Feng, J.; Camaioni, D. M.; Mei, D.; Hu, J. Z.; Zhao, C.; Lercher, J. A. Following Solid-Acid-Catalyzed Reactions by MAS NMR Spectroscopy in Liquid Phase—Zeolite-Catalyzed Conversion of Cyclohexanol in Water. *Angew. Chem., Int. Ed.* **2014**, *53*, 479−482.

(10) Andanson, J.-M.; Baiker, A. Exploring Catalytic Solid/Liquid Interfaces by *In Situ* Attenuated Total Reflection Infrared Spectroscopy. *Chem. Soc. Rev.* **2010**, *39*, 4571−4584.

(11) Bürgi, T.; Baiker, A. In Situ Infrared Spectroscopy of Catalytic Solid-Liquid Interfaces Using Phase-Sensitive Detection: Enantioselective Hydrogenation of a Pyrone over Pd/TiO_2. *J. Phys. Chem. B* **2002**, *106*, 10649−10658.

(12) Ferri, D.; Diezi, S.; Maciejewski, M.; Baiker, A. Alumina-Catalysed Degradation of Ethyl Pyruvate during Enantioselective Hydrogenation over Pt/Alumina and Its Inhibition by Acetic Acid. *Appl. Catal., A* **2006**, *297*, 165−173.

(13) Ferri, D.; Baiker, A. Advances in Infrared Spectroscopy of Catalytic Solid−Liquid Interfaces: The Case of Selective Alcohol Oxidation. *Top. Catal.* **2009**, *52*, 1323−1333.

(14) Aguirre, A.; Bonivardi, A. L.; Matkovic, S. R.; Briand, L. E.; Collins, S. E. ATR-FTIR Study of the Decomposition of Acetic Anhydride on Fosfotungstic Wells−Dawson Heteropoly Acid Using Concentration-Modulation Excitation Spectroscopy. *Top. Catal.* **2011**, *54*, 229−235.

(15) Leinweber, P.; Kruse, J.; Walley, F. L.; Gillespie, A.; Eckhardt, K.-U.; Blyth, R. I. R.; Regier, T. Nitrogen K-edge XANES − An Overview of Reference Compounds Used to Identify 'Unknown' Organic Nitrogen in Environmental Samples. *J. Synchrotron Radiat.* **2007**, *14*, 500−511.

(16) Marsh, A. L.; Burnett, D. J.; Fischer, D. A.; Gland, J. L. Benzene Intermediates and Mechanisms during Catalytic Oxidation on the Pt(111) Surface Using In-Situ Soft X-ray Methods. *J. Phys. Chem. B* **2003**, *107*, 12472−12479.

(17) Senanayake, S. D.; Stacchiola, D.; Evans, J.; Estrella, M.; Barrio, L.; Pérez, M.; Hrbek, J.; Rodriguez, J. A. Probing the Reaction Intermediates for the Water-Gas Shift over Inverse $CeO_x/Au(1\ 1\ 1)$ Catalysts. *J. Catal.* **2010**, *271*, 392−400.

(18) Morales, F.; de Groot, F. M. F.; Glatzel, P.; Kleimenov, E.; Bluhm, H.; Hävecker, M.; Knop-Gericke, A.; Weckhuysen, B. M. In Situ X-ray Absorption of $Co/Mn/TiO_2$ Catalysts for Fischer−Tropsch Synthesis. *J. Phys. Chem. B* **2004**, *108*, 16201−16207.

(19) Chantler, C. T. Detailed Tabulation of Atomic Form Factors, Photoelectric Absorption and Scattering Cross Section, and Mass Attenuation Coefficients in the Vicinity of Absorption Edges in the Soft X-ray (Z = 30−36, Z = 60−89, E = 0.1 keV−10 keV), Addressing Convergence Issues of Earlier Work. *J. Phys. Chem. Ref. Data* **2000**, *29*, 597−1048.

(20) Schreck, S.; Gavrila, G.; Weniger, C.; Wernet, P. A Sample Holder for Soft X-ray Absorption Spectroscopy of Liquids in Transmission Mode. *Rev. Sci. Instrum.* **2011**, *82*, 103101.

(21) Wernet, P.; Nordlund, D.; Bergmann, U.; Cavalleri, M.; Odelius, M.; Ogasawara, H.; Näslund, L.-Å.; Hirsch, T. K.; Ojamäe, L.; Glatzel, P.; et al. The Structure of the First Coordination Shell in Liquid Water. *Science* **2004**, *304*, 995−999.

(22) Huang, C.; Wikfeldt, K. T.; Tokushima, T.; Nordlund, D.; Harada, Y.; Bergmann, U.; Niebuhr, M.; Weiss, T. M.; Horikawa, Y.; Leetmaa, M.; et al. The Inhomogeneous Structure of Water at Ambient Conditions. *Proc. Natl. Acad. Sci. U. S. A.* **2009**, *106*, 15214−15218.

(23) Smith, J. D.; Cappa, C. D.; Wilson, K. R.; Messer, B. M.; Cohen, R. C.; Saykally, R. J. Energetics of Hydrogen Bond Network Rearrangements in Liquid Water. *Science* **2004**, *306*, 851−853.

(24) Achkar, A. J.; Regier, T. Z.; Wadati, H.; Kim, Y.-J.; Zhang, H.; Hawthorn, D. G. Bulk Sensitive X-ray Absorption Spectroscopy Free of Self-Absorption Effects. *Phys. Rev. B* **2011**, *83*, 081106(R).

(25) Gotz, M. D.; Soldatov, M. A.; Lange, K. M.; Engel, N.; Golnak, R.; Könnecke, R.; Atak, K.; Eberhardt, W.; Aziz, E. F. Probing Coster−Kronig Transitions in Aqueous Fe^{2+} Solution Using Inverse Partial and Partial Fluorescence Yield at the L-Edge. *J. Phys. Chem. Lett.* **2012**, *3*, 1619−1623.

DOI: 10.1021/jp512891t
J. Phys. Chem. C 2015, 119, 7738−7745

(26) Regier, T. Z.; Achkar, A. J.; Peak, D.; Tse, J. S.; Hawthorn, D. G. Dark Channel Fluorescence Observations Result from Concentration Effects Rather than Solvent-Solute Charge Transfer. *Nat. Chem.* **2012**, *4*, 765−766.
(27) Soldatov, M. A.; Lange, K. M.; Gotz, M. D.; Engel, N.; Golnak, R.; Kothe, A.; Aziz, E. F. On the Origin of Dips in Total Fluorescence Yield X-ray Absorption Spectra: Partial and Inverse Partial Fluorescence Yield at the L-Edge of Cobalt Aqueous Solution. *Chem. Phys. Lett.* **2012**, *546*, 164−167.
(28) Huse, N.; Wen, H.; Nordlund, D.; Szilagyi, E.; Daranciang, D.; Miller, T. A.; Nilsson, A.; Schoenlein, R. W.; Lindenberg, A. M. Probing the Hydrogen-Bond Network of Water via Time-Resolved Soft X-ray Spectroscopy. *Phys. Chem. Chem. Phys.* **2009**, *11*, 3951−3957.
(29) Meibohm, J.; Schreck, S.; Wernet, P. Temperature Dependent Soft X-ray Absorption Spectroscopy of Liquids. *Rev. Sci. Instrum.* **2014**, *85*, 103102.
(30) Nagasaka, M.; Hatsui, T.; Horigome, T.; Hamamura, Y.; Kosugi, N. Development of a Liquid Flow Cell to Measure Soft X-ray Absorption in Transmission Mode: a Test for Liquid Water. *J. Electron Spectrosc. Relat. Phenom.* **2010**, *177*, 130−134.
(31) Nagasaka, M.; Mochizuki, K.; Leloup, V.; Kosugi, N. Local Structures of Methanol−Water Binary Solutions Studied by Soft X-ray Absorption Spectroscopy. *J. Phys. Chem. B* **2014**, *118*, 4388−4396.
(32) Nagasaka, M.; Yuzawa, H.; Horigome, T.; Hitchcock, A. P.; Kosugi, N. Electrochemical Reaction of Aqueous Iron Sulfate Solutions Studied by Fe L-edge Soft X-ray Absorption Spectroscopy. *J. Phys. Chem. C* **2013**, *117*, 16343−16348.
(33) Nagasaka, M.; Yuzawa, H.; Horigome, T.; Kosugi, N. In Operando Observation System for Electrochemical Reaction by Soft X-ray Absorption Spectroscopy with Potential Modulation Method. *Rev. Sci. Instrum.* **2014**, *85*, 104105.
(34) Sugiyama, K.; Miura, H.; Nakano, Y.; Sekiwa, H.; Matsuda, T. Heterogeneous Hydration of Acrylonitrile over the Metal Oxide Catalysts in Liquid Phase. *Bull. Chem. Soc. Jpn.* **1986**, *59*, 2983−2989.
(35) Yamaguchi, K.; Matsushita, M.; Mizuno, N. Efficient Hydration of Nitriles to Amides in Water, Catalyzed by Ruthenium Hydroxide Supported on Alumina. *Angew. Chem., Int. Ed.* **2004**, *43*, 1576−1580.
(36) Roy, S. C.; Dutta, P.; Nandy, L. N.; Roy, S. K.; Samuel, P.; Pillai, S. M.; Kaushik, V. K.; Ravindranathan, M. Hydration of 3-Cyanopyridine to Nicotinamide over MnO_2 Catalyst. *Appl. Catal., A* **2005**, *290*, 175−180.
(37) Tamura, M.; Wakasugi, H.; Shimizu, K.-i.; Satsuma, A. Efficient and Substrate-Specific Hydration of Nitriles to Amides in Water by Using a CeO_2 Catalyst. *Chem.—Eur. J.* **2011**, *17*, 11428−11431.
(38) Tamura, M.; Satsuma, A.; Shimizu, K.-i. CeO_2-Catalyzed Nitrile Hydration to Amide: Reaction Mechanism and Active Sites. *Catal. Sci. Technol.* **2013**, *3*, 1386−1393.
(39) Hatsui, T.; Shigemasa, E.; Kosugi, N. Design of a Transmission Grating Spectrometer and an Undulator Beamline for Soft X-ray Emission Studies. *AIP Conf. Proc.* **2004**, *705*, 921−924.
(40) Ueda, K.; Okunishi, M.; Chiba, H.; Shimizu, Y.; Ohmori, K.; Sato, Y.; Shigemasa, E.; Kosugi, N. Rydberg−Valence Mixing in the C ls Excited States of CH_4 Probed by Electron Spectroscopy. *Chem. Phys. Lett.* **1995**, *236*, 311−317.
(41) Flesch, R.; Pavlychev, A. A.; Neville, J. J.; Blumberg, J.; Kuhlmann, M.; Tappe, W.; Senf, F.; Schwarzkopf, O.; Hitchcock, A. P.; Rühl, E. Dynamic Stabilization in $1\sigma_u \rightarrow 1\pi_g$ Excited Nitrogen Clusters. *Phys. Rev. Lett.* **2001**, *86*, 3767−3770.
(42) Aminpirooz, S.; Becker, L.; Hillert, B.; Haase, J. High Resolution NEXAFS Studies of Aromatic Molecules Adsorbed and Condensed on Ni(111). *Surf. Sci. Lett.* **1991**, *244*, L152−L156.
(43) Vall-llosera, G.; Gao, B.; Kivimäki, A.; Coreno, M.; Álvarez Ruiz, J.; de Simone, M.; Ågren, H.; Rachlew, E. The C 1s and N 1s Near Edge X-ray Absorption Fine Structure Spectra of Five Azabenzenes in the Gas Phase. *J. Chem. Phys.* **2008**, *128*, 044316.
(44) Hitchcock, A. P.; Tronc, M.; Modelli, A. Electron Transmission and Inner-Shell Electron Energy Loss Spectroscopy of CH_3CN, CH_3NC, CH_3SCN, and CH_3NCS. *J. Phys. Chem.* **1989**, *93*, 3068−3077.
(45) Ikeura-Sekiguchi, H.; Sekiguchi, T.; Kitajima, Y.; Baba, Y. Inner Shell Excitation and Dissociation of Condensed Formamide. *Appl. Surf. Sci.* **2001**, *169−170*, 282−286.
(46) Lessard, R.; Cuny, J.; Cooper, G.; Hitchcock, A. P. Inner-Shell Excitation of Gas Phase Carbonates and α,γ-Dicarbonyl Compounds. *Chem. Phys.* **2007**, *331*, 289−303.

DOI: 10.1021/jp512891t
J. Phys. Chem. C 2015, 119, 7738−7745